

AD _____

Award Number: DAMD17-01-1-0420

TITLE: Development of a Novel in-situ Telomere Length
Qualification System to Address Suitability of Telomerase
Inhibitor Therapy to Breast Cancer

PRINCIPAL INVESTIGATOR: Nicholas R. Forsyth, Ph.D.

CONTRACTING ORGANIZATION: The University of Texas Southwestern
Medical Center at Dallas
Dallas, TX 75390-9105

REPORT DATE: April 2004

TYPE OF REPORT: Annual Summary

PREPARED FOR: U.S. Army Medical Research and Materiel Command
Fort Detrick, Maryland 21702-5012

DISTRIBUTION STATEMENT: Approved for Public Release;
Distribution Unlimited

The views, opinions and/or findings contained in this report are
those of the author(s) and should not be construed as an official
Department of the Army position, policy or decision unless so
designated by other documentation.

20040903 049

REPORT DOCUMENTATION PAGEForm Approved
OMB No. 074-0188

Public reporting burden for this collection of information is estimated to average 1 hour per response, including the time for reviewing instructions, searching existing data sources, gathering and maintaining the data needed, and completing and reviewing this collection of information. Send comments regarding this burden estimate or any other aspect of this collection of information, including suggestions for reducing this burden to Washington Headquarters Services, Directorate for Information Operations and Reports, 1215 Jefferson Davis Highway, Suite 1204, Arlington, VA 22202-4302, and to the Office of Management and Budget, Paperwork Reduction Project (0704-0188), Washington, DC 20503

1. AGENCY USE ONLY (Leave blank)		2. REPORT DATE April 2004	3. REPORT TYPE AND DATES COVERED Annual Summary (1 Apr 2001 - 31 Mar 2004)	
4. TITLE AND SUBTITLE Development of a Novel in-situ Telomere Length Qualification System to Address Suitability of Telomerase Inhibitor Therapy to Breast Cancer			5. FUNDING NUMBERS DAMD17-01-1-0420	
6. AUTHOR(S) Nicholas R. Forsyth, Ph.D.				
7. PERFORMING ORGANIZATION NAME(S) AND ADDRESS(ES) The University of Texas Southwestern Medical Center at Dallas Dallas, TX 75390-9105 E-Mail: Nicholas.forsyth@utsouthwestern.edu			8. PERFORMING ORGANIZATION REPORT NUMBER	
9. SPONSORING / MONITORING AGENCY NAME(S) AND ADDRESS(ES) U.S. Army Medical Research and Materiel Command Fort Detrick, Maryland 21702-5012			10. SPONSORING / MONITORING AGENCY REPORT NUMBER	
11. SUPPLEMENTARY NOTES				
12a. DISTRIBUTION / AVAILABILITY STATEMENT Approved for Public Release; Distribution Unlimited				12b. DISTRIBUTION CODE
13. ABSTRACT (Maximum 200 Words) The ability to predetermine therapeutic intervention times following tumor resection would be invaluable to patient well being and clinical resources. We sought to determine if we could establish a methodology where in vivo tumor telomere length could be established using in situ hybridisation as a quantitative tool. This technique would require development, validation, and application to a model system. A three dimensional technique to measure telomere length was established. This technique was applied to breast cancer derived tumor cell lines thereby establishing technique, methodology, and validity. In vivo application was established using both a readily available tissue source and tumors derived from tumorigenic breast cancer cell lines. Combining the approach to breast cancer cell lines we were then able to approximate at required times of telomerase inhibition before driving the cells into telomere-driven replicative senescence. This technique represents an important development in the ability to measure telomere length in vivo and ultimately could become appropriate for clinical application.				
14. SUBJECT TERMS Telomerase, Telomeres, Q-FISH				15. NUMBER OF PAGES 19
				16. PRICE CODE
17. SECURITY CLASSIFICATION OF REPORT Unclassified	18. SECURITY CLASSIFICATION OF THIS PAGE Unclassified	19. SECURITY CLASSIFICATION OF ABSTRACT Unclassified	20. LIMITATION OF ABSTRACT Unlimited	

Table of Contents

Cover.....	1
SF 298.....	2
Table of contents.....	3
Introduction.....	4
Body.....	5
Key Research Accomplishments.....	7
Reportable Outcomes.....	7
Conclusions.....	8
References.....	9
Appendices.....	A1 - 10

Introduction

Cells contain multiple copies of the TTAGGG hexameric DNA repeat sequences called telomeres (1). Found at the end of linear chromosomes, telomeres and telomere-associated proteins provide a protective end capping structure (2). The lengths of telomeres have also been shown to decrease with time and age (3). The end replication problem of DNA replication is the mechanism responsible for this shortening; this is described by the inability of DNA polymerases to copy all the way to the end of a linear molecule (4). Progressive telomere shortening with cell divisions results in replicative senescence (5). The mechanism termed replicative senescence is the means whereby normal cells have a controlled lifespan after which cellular proliferation ceases. The replicative senescence mechanism is thought to occur as a response to the presence of critically short telomere(s). These critically short telomere(s) in turn are thought to instigate a DNA-damage response, which prevents further proliferation through upregulation of effector molecules (6).

Maintenance of telomeres has been shown to involve telomerase activity, which acts as a reverse transcriptase to add base pairs to the ends of chromosomes (7). It has been proposed that an immortalized cell emerges from a stage called crisis, characterized by a period of genomic instability, when telomerase or another mechanism to maintain telomere stability is activated (8). Once telomerase is activated it elongates and stabilizes telomere length and permits continued cell division. Most cancer cells have been shown to contain short but stable telomeres compared to parental cells. Beside germ line and stem cells of renewal tissues, other cells having telomerase activity are cancer cells (90% of those tested) (9). Telomerase activity can be determined using a standard PCR-based assay with a labeled primer and cell extracts (10).

Telomerase has been shown to become active early in breast cancer progression (11-15). This early activation will therefore maintain the majority of the cancer cells telomere population (46 pairs) at a level beyond the critical minimum seen in senescence and crisis. Immortalized breast cancer cell lines in culture tend to have mean telomere lengths in the range of 3-5 kb. This short length leads to the implication that the telomeres have been stabilized but not greatly elongated. We sought to analyze cell lines derived from breast cancers to establish what TRF kb (traditional electrophoresis value) and Q-FISH values they possessed and then to treat the cells with telomerase inhibitors. This generates a predictive capacity relating true telomere length to telomerase inhibition times.

With this approach we were able to generate value correlations for telomere Q-FISH vs. telomeric kb (TRF). This in turn enables in vivo tissue/tumor Q-FISH analysis and telomere length prediction. The results show that true telomere length can be determined by Q-FISH and strongly suggest that when combined with telomerase inhibition required therapy time should be predictive.

Body

The first year's statement of work was summarized by the statement 'The direct visualization of telomeric and centromeric signals from Human Mammary Epithelial Cells (HMECs) via Q-FISH, in a 2-D cell culture environment'. In order to achieve this we cultured and characterized two cell lines, HME13 and HME17. We determined the telomere shortening rates by standard electrophoretic techniques (TRF, Telomere Restriction Fragment analysis) and compared differences between cells cultured in low physiologic (2-5%) and room (21%) oxygen. With this data we showed variation in telomere shortening rates and protein regulation concurrent with the onset of replicative senescence. We had hoped to use our characterized HMEC lines to generate a correlation between Q-FISH values and telomeric electrophoresis values. However, despite repeated attempts we were not successful in recovering cells which had been previously frozen back. Our cell yields were low and insufficient for the generation of metaphase spreads. To overcome this problem we developed a model of quantification utilizing a panel of breast cancer-derived tumor cell lines; MDA MB 231, MDA MB 468, MCF7, and HCC1937. The calculated telomere lengths for these cell lines and a representative gel image are shown in A1.

Previously we had reported difficulties in applying a centromeric probe for telomeric normalization. A secondary difficulty we encountered was when using DAPI signal as the telomere intensity normalization. We encountered a ≥ 5 -fold variation in intensity which we felt was unreasonably high from seemingly homogenous cell populations. To investigate this we used a series of different treatments and processing steps. Pepsin is used to digest cellular proteins with in situ hybridization and we reasoned that our observed variations could be due to incomplete digestion. To address this we tested a number of conditions including no pepsin, a 95⁰TE (ph 7) pre-denaturation step, and three pepsin concentrations (0.1, 1, and 10 mg/ml). No difference was observed between the three pepsin concentrations and the middle value was not included after the first test. Over thirty interphase nuclei were analyzed for each treatment, this was repeated in triplicate. The analysis protocol is detailed in A2. In each instance the summed telomere intensity was normalized for exposure, corrected for background variations and divided by the summed DAPI exposure to generate a normalized telomere intensity value termed a TDU (Telomere/DAPI Unit). This was calculated via the formula $TTI - [(TBI - TTI) / (TNA - TTA) \times TTA]$ where TTI= total telomeric intensity, TBI=total background intensity, TNA=total nuclear area, and TTA=total telomeric area. The outcomes are expressed in A3. These outcomes showed us that pepsin had no effect on the accessibility of telomeric probe and led us to discontinue its use in the telomere hybridization protocol. A full protocol is detailed in A2.

We were then able to apply our refined protocol to our panel of breast tumor lines (A1). We achieved a high level of quantification with this approach which is illustrated in A4. This validated our approach in 2-D and enabled us to calculate the true telomere value for each of the panel of tumor lines.

The second year's statement of work was summarized by the statement 'Direct visualization of telomeric and centromeric signal from HMEC through Q-FISH in a 3-D cell culture environment.' Due to the difficulties in recovering the HME cell lines from freeze backs we developed a system which took advantage of the tumorigenic properties of MDAMB 231. We inoculated the opposite flanks of nude mice with either the parental cell line or a line with artificially elongated telomeres (A5). Tumors were resected after 21 days, fixed, embedded in paraffin, and sectioned at our predetermined optimal thickness of 10 μ m. Full protocols for telomere staining and intensity analysis are detailed in A6. Telomere analysis of our tumors showed that we retained our quantitative capacity in 3-D and also enabled us to develop a telomere shortening profile where TDU could be directly correlated to kb of true telomere (A7).

We established that a kb of telomere was reflected by 0.00064 TDU. With the establishment of this relationship we felt confident of our capacity to predict telomere length of tissues *in vivo*.

The third and final year's statement of work was summarized by the statement 'Telomeric analysis of breast tumor sections to determine effectiveness of telomerase inhibitor adjuvant therapy'. Although we had demonstrated the ability to quantitatively distinguish between 5 and 12 kb long telomeres we felt it advisable to apply our technique to an *in vivo* situation. In collaboration with the Plastic Surgery Research department at UTSW Medical Center we established a normal skin bank from breast and abdominal reduction surgery's. We collected approximately 30 patient samples with ages spanning 0-75 yrs. For the purposes of analysis samples were binned in decade groupings and ranked according to the mean age of the individual bin. Due to the inherent variability in telomere length this represents a more measured representation than those based on individuals within a wider population (X). We performed analysis as described in A6 and used this to generate a telomere shortening with age profile. Our technique illustrated that telomeres do shorten with age *in vivo*. To further characterize our samples we analyzed telomeres from the adjoining dermis and found that they to shorten with age. Combined analysis from both data sets is shown in A8. Utilizing our TDU/kb conversion we were able to generate real kb values for both the epidermis and the dermis (A9). We found that telomere shortening rates were approximately 1.5X greater in the epidermal compartment of skin than in the dermal compartment. Telomeres in the dermal compartment were also shorter throughout life than those seen in the epidermis. These results suggest strongly that *in vivo* telomere lengths could be calculated for tumors following resection. It remained to be determined how effective telomerase inhibitors would be in driving immortal breast cancer cell lines into senescence.

To study the effectiveness of telomerase inhibition on breast cancer cell lines we again utilized the MDAMB 231 cell line. We first determined an effective non toxic treatment dose of the telomerase inhibition drug GRN719 which we obtained from Geron, Menlo Park, CA. The non-toxic dose was 0.5 μ M, this required media addition every 3 days to ensure complete telomerase activity quenching. Continual treatment of the drug was performed for 50 days to determine if telomere shortening would occur. We established that inhibition of telomerase activity resulted in 35 bp/PD of telomere shortening. This shortened telomeres from 5 kb to a final length of 3.9 kb. Based on our earlier determination of the true telomere length of MDAMB 231 cells a further shortening of 1.3 kb (37.5 PD or 44 days) would be required before telomere-directed senescence occurred. Based on the observed MDAMB 231 telomere shortening rates and assuming consistency between cell lines we can formulate predictions of required treatment times of MDA MB 468 (23 PD or 35 days), MCF7 (37 PD or 55 days), and HCC1937 (43 PD or 65 days). This suggests that telomerase inhibition therapies would be successful without requiring long term treatments in removing telomerase positive tumor cells following breast cancer resection.

The development of the Q-FISH technology represents an important advancement in the ability to visualize and quantify telomeres *in vivo*. This approach should help to understand, determine, and assist in application of telomerase inhibitors following resection of breast cancer tumors.

Key Research Accomplishments

Original Statement Task 1. Direct visualization of telomeric and centromeric signal from Human Mammary Epithelial Cells (HMEC) through Q-FISH in a 2-D cell culture environment.

Months 1-12.

- Quantification and linearity of Q-FISH established with breast cancer cell lines MDA MB 231, MDA MB 468, MCF7, and HCC1937.
- DAPI determined to be a more robust normalization than a centromeric probe.
-

Original Statement Task 2. Direct visualization of telomeric and centromeric signal from Human Mammary Epithelial Cells (HMEC) through Q-FISH in a 3-D cell culture environment.

Months 12-24.

- Development of 3-D model based on tumors with preset telomere lengths.
- Quantification established with 3-D tumor model using DAPI as a normalization.

Original Statement Task 3. Telomeric analysis of breast tumor sections to determine effectiveness of telomerase inhibitor adjuvant therapy.

Months 24-36.

- Quantification of *in vivo* model established using breast reduction and abdominal skin.
- Effectiveness of telomerase inhibition on breast cancer lines established.
- Model of required telomerase inhibition treatment time established using predetermined true telomere lengths.

Reportable Outcomes

Publications

Forsyth, N. R and Shay J. W. Telomere shortening with age in normal human skin. Manuscript in preparation.

Forsyth, N. R., Shay, J. W. and Wright, W. E. Lagomorphs do not exhibit telomere-directed aging in vitro. Manuscript in review. Experimental Cell Research.

Forsyth N. R., Morales C. P., Boman B., Kopelovich L., and Shay J. W. Spontaneous immortalization of Clinically normal Colon-derived fibroblasts from a Familial Adenomatous Polyposis (FAP) Patient. Manuscript in press. Neoplasia

Forsyth, N. R., Evans, A. P., Shay, J. W. and Wright, W. E. Developmental differences in the immortalization of lung fibroblasts by telomerase. Aging Cell 2 (5): 235-243. 2003

Forsyth, N. R., Wright, W. E., and Shay, J. W. Telomerase and differentiation in multicellular organisms: Turn it off, turn it on, and turn it off again. Differentiation 69 (4-5), 188-197. 2002

Abstracts

Forsyth, N. R., Evans, A. P., Shay, J. W., Wright, W. E. Oxygen levels can affect telomerase elongation rates and maintenance telomere lengths. AACR Telomere and Telomerase Conference, San Francisco, CA. December 2002.

Forsyth, N. R., LaRue, D. M., Wright, W. E., Shay, J. W. Development of a Novel *in-situ* Telomere Length Quantification System to Address Suitability of Telomerase Inhibitor Therapy to Breast Cancer Following Corrective Surgery. Breast Cancer Research Program Annual Meeting. Era of Hope 2002. Orlando, FLA. September 2002.

Forsyth, N. R., Shay, J. W., Wright, W. E. Appropriate culture conditions extend lifespan of WI38 cells enabling hTERT immortalization. Keystone Symposium entitled 'Genetics and Genomics of Senescence and Cancer. Jan 2002.

Conclusions

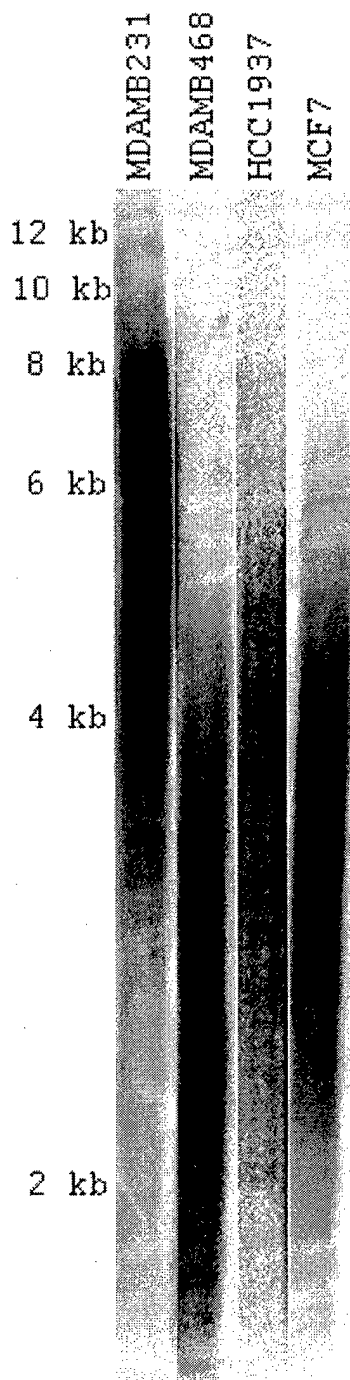
In summary we have developed a novel system which incorporates fluorescence microscopy and in situ hybridisation to quantify the lengths of telomeres *in vivo*. This has involved a number of technical challenges as well as adaptations to the best available reagents. In the process of accomplishing our original task statements we have modified our telomeric normalization from a centromeric probe to DAPI, adjusted a controlled 3-D environment from HMECs to a more manageable breast cancer tumor model, applied our methodology to an *in vivo* model with very positive results, and finally generated a predictive basis for telomerase inhibition of breast cancer tumor lines.

References

1. E. H. Blackburn, *Nature* **350**, 569 (1991).
2. J. D. Griffith *et al.*, *Cell* **97**, 503 (1999).
3. C. B. Harley, A. B. Futcher, C. W. Greider, *Nature* **345**, 458 (1990).
4. A. M. Olovnikov, *Izv Akad Nauk Ser Biol*, 504 (Jul-Aug, 1995).
5. N. R. Forsyth, A. P. Evans, J. W. Shay, W. E. Wright, *Aging Cell* **2**, 235 (Oct, 2003).
6. H. Takai, A. Smogorzewska, T. de Lange, *Curr Biol* **13**, 1549 (Sep 2, 2003).
7. W. E. Wright, D. Brasiskyte, M. A. Piatyszek, J. W. Shay, *Embo J* **15**, 1734 (1996).
8. J. W. Shay, W. E. Wright, *Exp Cell Res* **184**, 109 (1989).
9. J. W. Shay, S. Bacchetti, *Eur J Cancer* **33**, 787 (Apr, 1997).
10. W. E. Wright, J. W. Shay, M. A. Piatyszek, *Nucleic Acids Res* **23**, 3794 (1995).
11. K. A. Kolquist *et al.*, *Nat Genet* **19**, 182 (1998).
12. T. Sugino *et al.*, *Int J Cancer* **69**, 301 (1996).
13. E. Hiyama *et al.*, *J Natl Cancer Inst* **88**, 116 (1996).
14. A. K. Bednarek, A. Sahin, A. J. Brenner, D. A. Johnston, C. M. Aldaz, *Clin Cancer Res* **3**, 11 (1997).
15. S. Nawaz, T. L. Hashizumi, N. E. Markham, A. L. Shroyer, K. R. Shroyer, *Am J Clin Pathol* **107**, 542 (1997).

Appendices

A1



Telomere Lengths of Breast Cancer Cell Lines. Telomeres from a panel of four breast tumor cell lines were analyzed to determine their mean lengths. DNA was extracted, digested with a cocktail of restriction enzymes, separated using gel electrophoresis, and quantified using ImageQuant software. These cell lines were MDAMB 231 (4.9 kb), MDAMB 468 (3.1 kb), HCC1937 (3.8 kb), and MCF7 (3.6 kb).

A2

Telomere Staining and Image Capture in 2-D. Metaphase spreads were prepared and dropped onto slides as described in detail elsewhere. Dropped slides were then kept in a cool, dry environment before telomere staining. Slides were first rehydrated in PBS for 15 min before fixation in 4% Formaldehyde/PBS for 2 min. Following fixation slides were processed through 1 min sequential washes in PBS, 25%, 50% and 100% ethanol. After a 10 min air dry, telomere-directed amidate probe (T_2AG_3)₃ (2ng/ml, diluted in 70% formamide buffer solution, pH7.8 and 10% Blocking reagent, pH7.5 (Sigma cat# 1096176)) was applied to the slide, under a coverslip, which was then denatured at 95°C for 15 min prior to 16 hrs hybridization at 37°C in a humidified incubator. Slides were then washed in formamide buffer for 15 min, repeated four times, and 0.025% Tween 20/PBS for 5 min, repeated 4 times. Sequential washes in PBS, 25%, 50% and 100% Ethanol, and a 10 min air dry were performed before incubating the slide in 1µg/ml Dapi/Methanol for 15 min at 37°C. After a brief wash in methanol samples were mounted in Vectashield (Vector Laboratories, Burlingame, CA). All images were captured with a Hamamatsu Orca camera, 12 bit color depth, mounted on an Axioplan 2 (Zeiss) fluorescence microscope, through a 100X 1.4Na Pan-APOCHROMAT (Zeiss) oil immersion objective using Openlab 3.01 (Improvision).

Image analysis

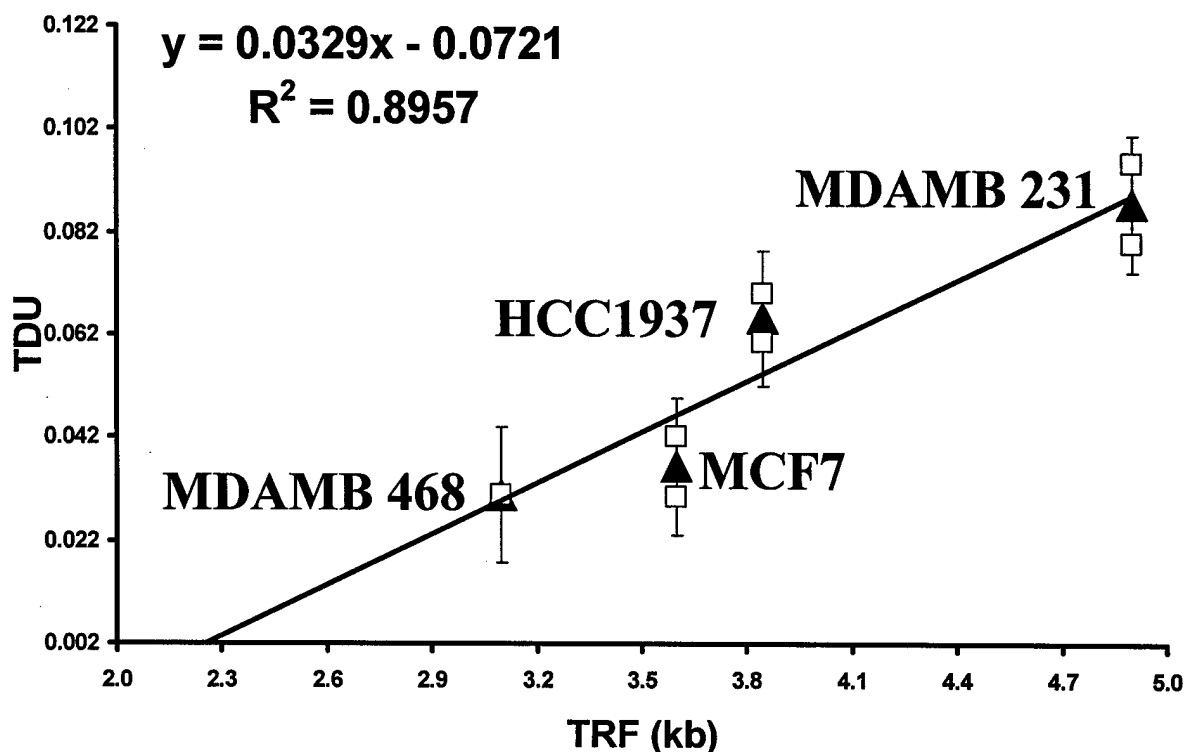
Image analysis was performed using Volocity (Improvision). Images were captured using the DAPI channel for our normalization standard and the Rhodamine channel for the telomere stain. Exposure times were recorded throughout and were calculated to be 75% of the saturation exposure. Images were first adopted, sorted according to channel and combined into an image sequence. Each field was cropped down to individual nuclei prior to analysis which was performed using Classifier modules. Total DAPI intensity and summed telomere intensity was recorded for each individual nucleus. Telomeres were then normalized for exposure to 1 second, corrected for background exposure using the formula; $TTI - [(TBI - TTI) / (TNA - TTA) \times TTA]$ where TTI= total telomeric intensity, TBI=total background intensity, TNA=total nuclear area, and TTA=total telomeric area. Corrected, summed telomere signal was then divided by exposure corrected DAPI signal (to 10 ms) to yield a TDU value for each nucleus. This process was repeated for each nucleus in the field and an average value generated from all TDU values.

A3

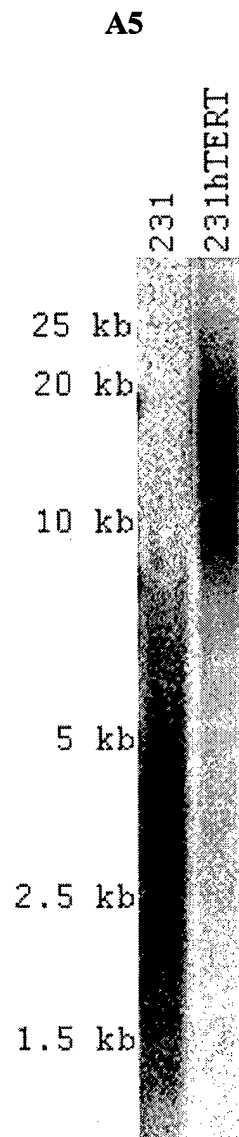
	D	0.1mg/ml	10mg/ml	90°TE
SD/Mean	0.50	0.55	0.81	0.35
	0.46	0.48	0.44	0.60
	0.48	0.65	0.42	0.54
sum	1.4	1.7	1.7	1.5
sum/3	0.48	0.56	0.56	0.50
overall rank	1	3	4	2

Variations within TDU Following Different Treatments. In order to achieve lower variations in TDU values within a population cells were treated with different agents prior to hybridization. A full protocol is described in A3. D = No treatment, 0.1 mg/ml and 10 mg/ml indicate pepsin concentrations, 90°TE indicates a 15 min incubation in 90°TE (ph7) prior to hybridization. Values are expressed as the standard deviation from the mean. The overall rank is attributed to the average of the sum of the three repeats. We find that there is very little difference between each of the treatments. This leads us to conclude that pepsin has no effect on the access of telomere probes to telomeric DNA.

A4



TRF vs. TDU. In order to establish quantification of our optimized telomere staining protocol we analyzed TDU vs. kb in four tumor lines. Approximately 25 nuclei were analyzed for each tumor line; analysis was performed for each sample in duplicate. Individual sample points are indicated by open squares, the mean values are detailed by solid triangles. The linear regression based on the solid trendline indicates an intercept on the X axis at 2.3 kb. This linearity suggests a common X region of 2.3 kb. The X region is comprised of subtelomeric DNA which is not digested by restriction enzymes and is included in telomere quantification (Steinert S, personal communication). The TDU value is an expression of total true telomere and does not include X region. This indicates that the true telomere lengths for MDAMB 231, MDAMB 468, MCF7, and HCC1937 are 2.6 kb, 0.8 kb, 1.3 kb, and 1.5 kb respectively. This establishes our quantification protocol in 2-dimensions.



MDAMB 231 Artificially Elongated Telomeres. In order to establish 3-D telomere analysis tumors were generated using cells with short (231) and long (231hTERT) telomeres.

A6

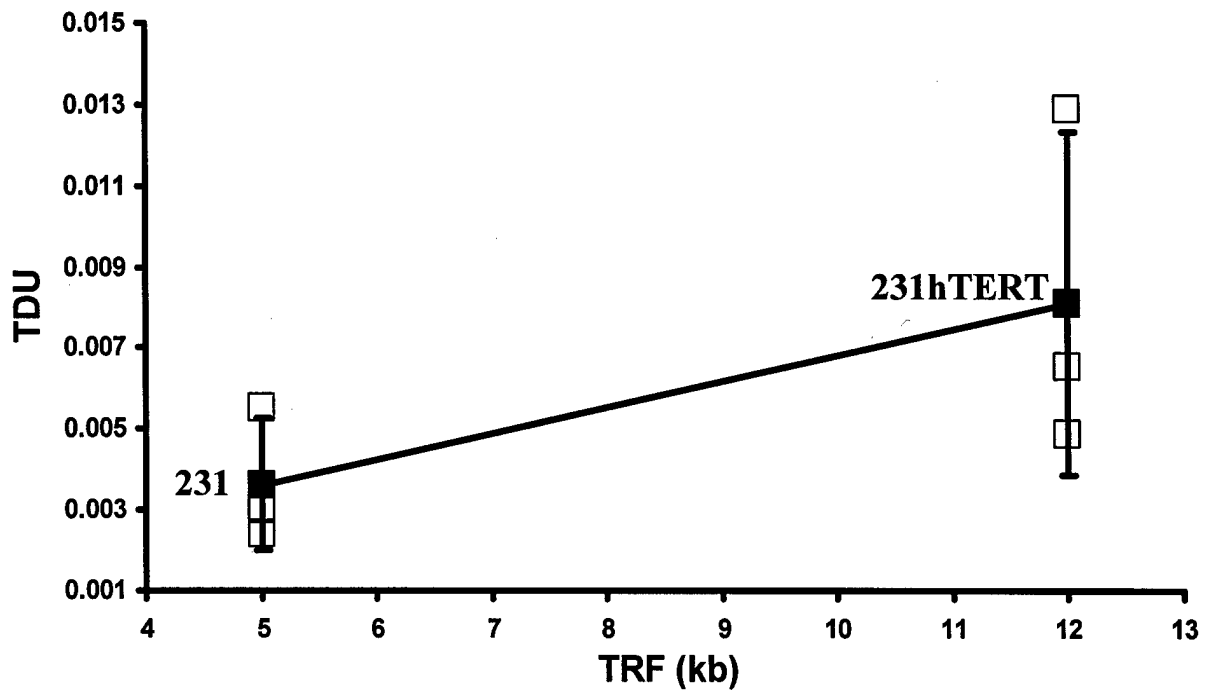
Telomere Staining and Image Capture in 3-D

Slides were first deparaffinized by melting at 65°C for 30 min. This was followed by two 10 min washes in fresh xylene, two 2 min 100% Ethanol washes, one PBS wash (1 min) and two brief washes in distilled water. Antigen retrieval was performed in 10mM sodium citrate for 30 min at 80°C followed by 1 min sequential washes in PBS, 25%, 50% and 100% ethanol. Following a 10 min air dry, telomere-directed amidate probe (T_2AG_3)₃ (2ng/ml, diluted in 70% formamide buffer solution, pH7.8 and 10% Blocking reagent, pH7.5 (Sigma cat# 1096176)) was applied to the slide, under a coverslip, which was then denatured at 95°C for 15 min prior to 16 hrs hybridization at 37°C in a humidified incubator. Slides were then washed in formamide buffer for 15 min, repeated four times, and 0.025% Tween 20/PBS for 5 min, repeated 4 times. Sequential washes in PBS, 25%, 50% and 100% Ethanol, and a 10 min air dry were performed before incubating the slide in 1µg/ml Dapi/Methanol for 15 min at 37°C. After a brief wash in methanol samples were mounted in Vectashield (Vector Laboratories, Burlingame, CA). All images were captured with a Hamamatsu Orca camera, 12 bit color depth, mounted on an Axioplan 2 (Zeiss) fluorescence microscope, with a motorized z-stage, through a 100X 1.4Na Pan-APOCHROMAT (Zeiss) oil immersion objective using Openlab 3.01 (Improvision). Images were captured with a two channel (DAPI and Rhodamine) automation where exposure times were set at 75% of the Automatic Exposure function as determined at the central plane of the section. Full size image capture, 1280 X 1024 was performed utilizing 0.4µm z-slice spacing.

Image analysis

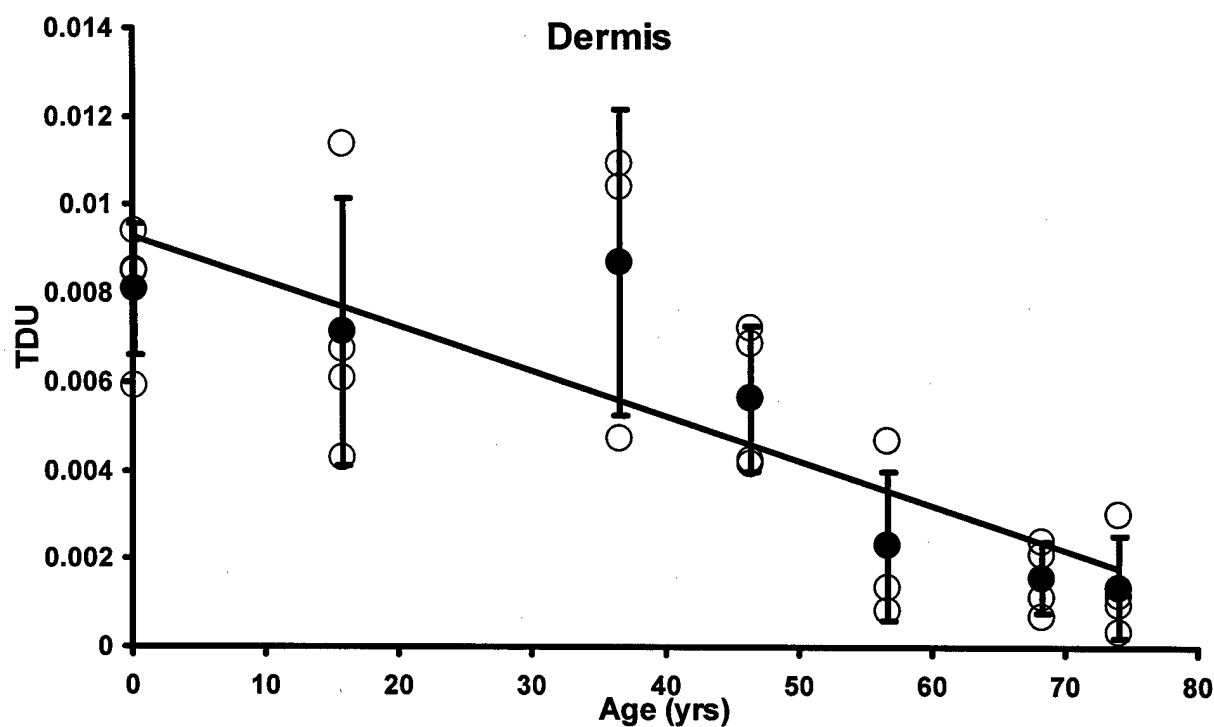
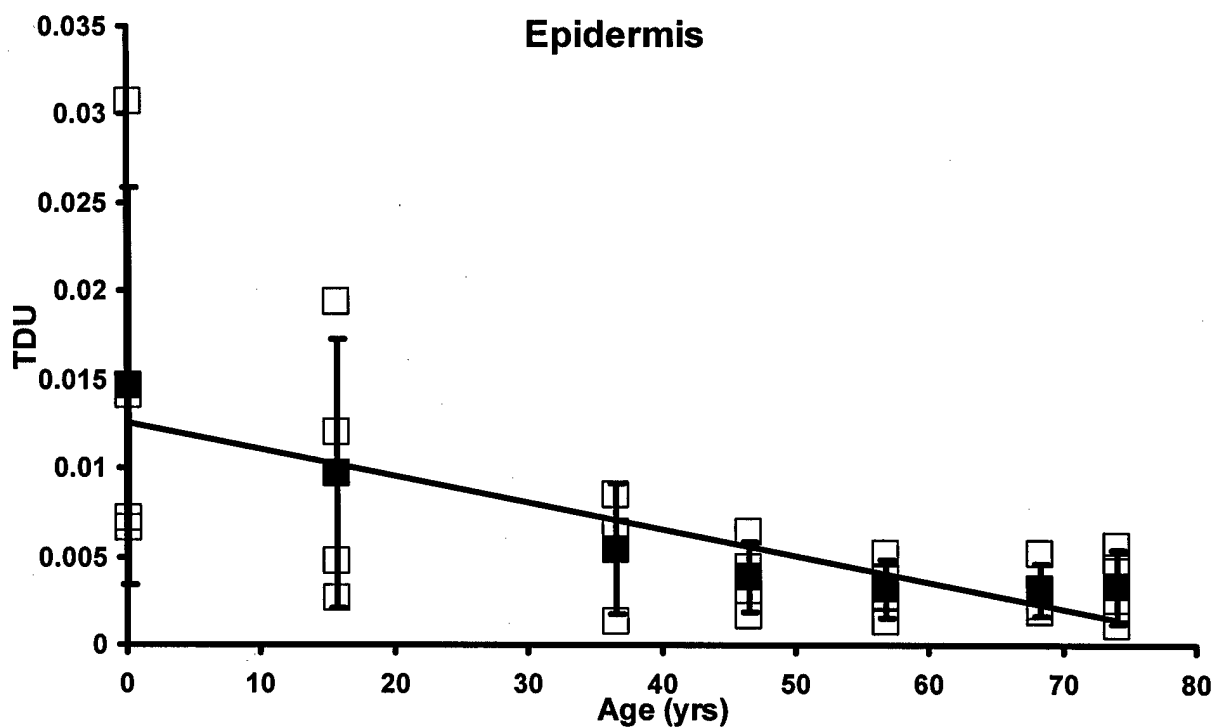
Image analysis was performed using Volocity (Improvision). Images were first adopted, sorted according to channel and transformed individually into 3-D volumes. Separate volumes were then combined into an image sequence, cropped into 512 X 512, x-y dimensions, images and processed using nondegradative iterative deconvolution to reassign or remove displaced photons based on measured point spread function algorithms specific for each channel. We determined 160 iterations to be necessary for sufficient resolution and photon reassignment in telomere analysis. Typically deconvolution of a 3-D image sequence requires 6-8 hrs. Following denconvolution images were converted to 16 bit and analysis was performed using Classifier modules. DAPI classifier was generated to select and measure all nuclei within an image. A telomere classifier was then generated and applied to the entire field and all identified objects measured. Using session arithmetic each identified nucleus was isolated and combined with the entire telomere field to positively identify colocalizing objects. Telomeres were then summed, normalized for exposure to 1 second, corrected for background exposure using the formula; $TTI - [(TBI - TTI) / (TNA - TTA) \times TTA]$ where TTI= total telomeric intensity, TBI=total background intensity, TNA=total nuclear area, and TTA=total telomeric area. Corrected, summed telomere signal was then divided by exposure corrected DAPI signal (to 10 ms) to yield a TDU value for each nucleus. This process was repeated for each nucleus in the field and an average value generated from all TDU values.

A7



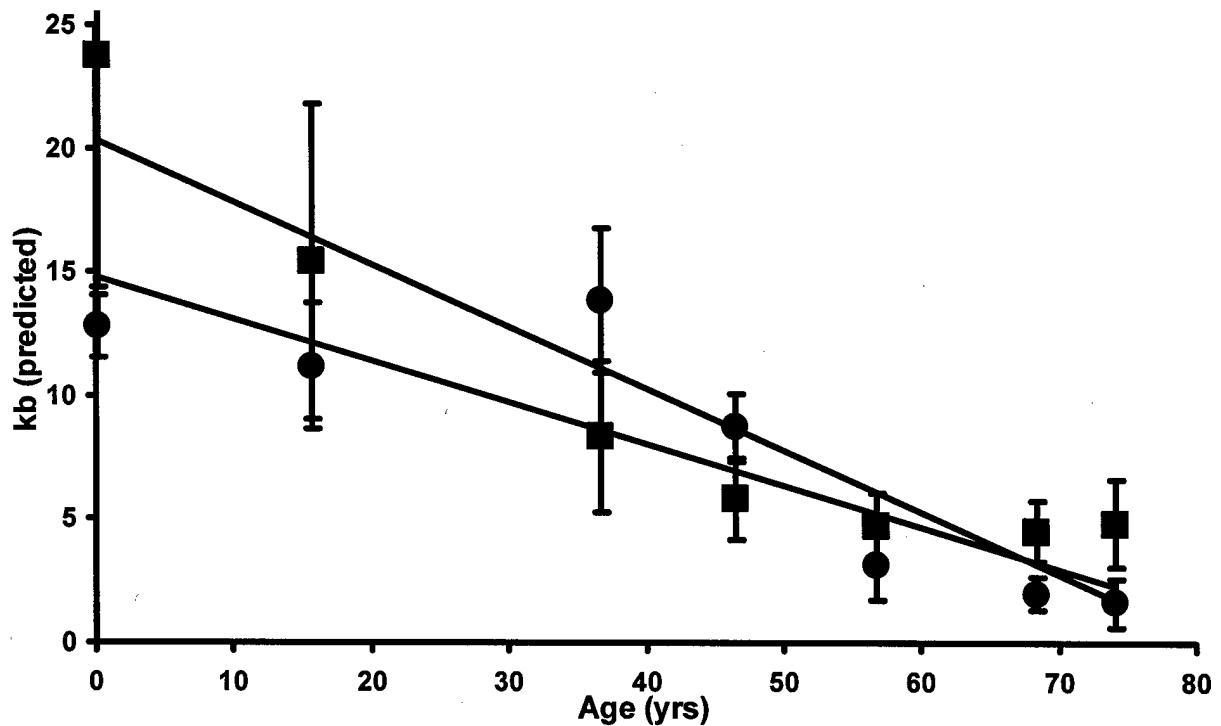
231 vs. 231hTERT Tumor Analysis. Individual analysis for each sample is represented by open squares. Repeated analysis was performed for each sample and the means of these repeats are shown by solid black squares. Error bars represent the SD for each sample grouping. The linear regression of the trendline is $y = 0.0006x + 0.0004$, where $y = \text{TDU}$ and $x = \text{kb}$. This generates in turn a TDU/kb value of 0.00064.

A8



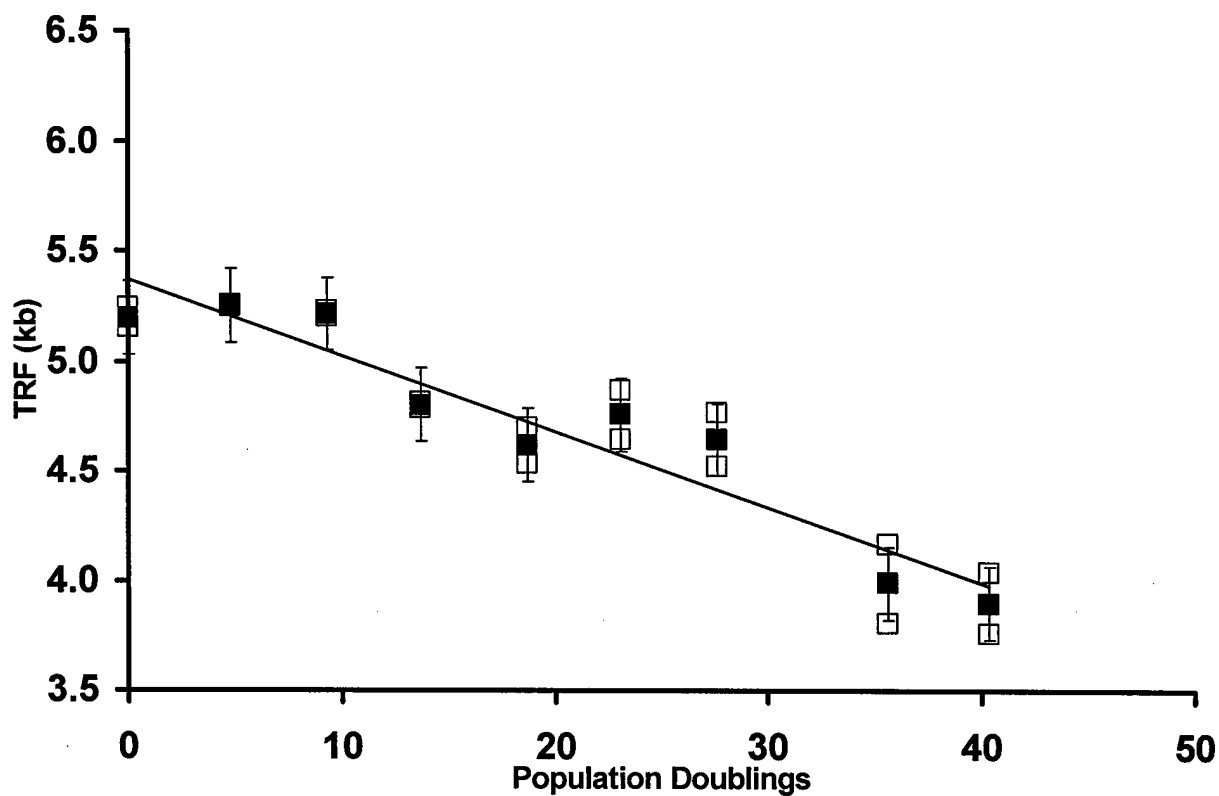
Telomere Shortening with Age. Individual samples are plotted as open symbols, mean values are plotted as closed symbols. Epidermis regression $y = -0.00015x + 0.013$, $R^2 = 0.87$, $R = 0.93$. Dermis regression $y = -0.0001x + 0.0093$, $R^2 = 0.75$, $R = 0.86$. Error bars represent the SD within each binned age grouping.

A9



Calculated Telomere Shortening Rates with Age. Epidermal and Dermal telomere lengths for each binned decade grouping are indicated by the solid squares and circles, respectively. These values indicate that epidermal telomeres have a mean telomere length of approximately 20 kb at birth and 5 kb in the elderly. This translates into a negative regression of 252 bp/year, $R^2 = 0.87$, $R = 0.93$. The dermal layer of skin has an initial length of 13 kb and an elderly length of 2 kb with a shortening rate of 168 bp/year, $R^2 = 0.75$, $R = 0.87$.

A10



Telomere Shortening with Telomerase Inhibition. Continued treatment of MDAMB 231 cells with GRN719 resulted in 35 bp/PD telomere shortening. Open squares indicate individual samples; closed squares indicate means of individual samples.